Металлофиз. новейшие технол. / *Metallofiz. Noveishie Tekhnol.*
2018, т. 40, № 10, сс. 1387–1399 / DOI: 10.15407/mfint.40.10.1387
Оттиски доступны непосредственно от издателя
Фотокопирование разрешено только
в соответствии с лицензией

ФИЗИКО-ТЕХНИЧЕСКИЕ ОСНОВЫ ЭКСПЕРИМЕНТА И ДИАГНОСТИКИ

PACS numbers: 46.40.Cd, 62.25.Jk, 62.30.+d, 68.37.Tj, 81.15.Gh, 81.40.Ef, 81.70.Cv

Scanning Acoustic Microscopy of Annealing Effects for Aluminium Thin Film Deposited on Silicon Substrate

Chafia Atailia, Lakhdar Deboub, Amar Boudour, and Youcef Boumaiza

Badji Mokhtar University,
Faculty of Sciences, Department of Physics,
Laboratory of Elaboration and Analysis of Materials,
B.P. 12, CP 23000 Annaba, Algeria

Scanning acoustic microscope (SAM) has proved to be a powerful new technique for investigation and characterization of mechanical properties of materials, especially, the opaque ones. Non-destructive measurements can be carried out using SAM in the vicinity of materials' surfaces or relatively deeper away from them. The present work is focussed on the effects of annealing on mechanical properties of samples composed of an Al layer (10 μm) on Si substrate. Combining the results obtained from the so-called acoustic signature and acoustic images of the Al/Si interface with those from the lateral and longitudinal waves (Rayleigh speeds), it is possible to deduce that the best homogeneous adhesion is obtained after annealing at 500°C.

Key words: non-destructive testing, scanning acoustic microscope, mechanical properties, annealing effects, thin Al/Si films.

Сканівний акустичний мікроскоп (САМ) є потужнім новим інструментом для дослідження та визначення механічних властивостей матеріялів, особливо непрозорих. САМ уможливлює проводити неруйнівні дослідження матеріялів як поблизу поверхні, так і на деякій віддалі від неї углиб зразка. Робота стосується вивчення впливу відпалу на механічні властивості зразків, що складаються з шару Al (10 мкм) на підложжі з Si. Поєднуючи результати, одержані з так званої акустичної сиґнатури й акустичних зображень інтерфейсу Al/Si з використанням поперечних і

Corresponding author: Amar Boudour
E-mail: amiredyoune@gmail.com

Citation: Chafia Atailia, Lakhdar Deboub, Amar Boudour, and Youcef Boumaiza, Scanning Acoustic Microscopy of Annealing Effects for Aluminium Thin Film Deposited on Silicon Substrate, *Metallofiz. Noveishie Tekhnol.*, **40**, No. 10: 1387–1399 (2018), DOI: 10.15407/mfint.40.10.1387.

поздовжніх хвиль (Релейових швидкостей), можна зробити висновок, що найліпша гомогенна адгезія реалізується після відпалу за 500°C.

Ключові слова: неруйнівна діягностика, сканівний акустичний мікроскоп, механічні властивості, ефекти відпалу, тонкі плівки Al/Si.

Сканирующий акустический микроскоп (САМ) является мощным современным инструментом для исследования и определения механических свойств материалов, особенно непрозрачных. САМ позволяет проводить неразрушающие исследования материалов как вблизи их поверхности, так и на некотором расстоянии от неё вглубь образца. Работа посвящена изучению влияния отжига на механические свойства образцов, состоящих из слоя Al (10 мкм) на подложке из Si. Объединяя результаты, полученные на основании измерений так называемой акустической сигнатуры и акустических изображений интерфейса Al/Si с использованием поперечных и продольных волн (скоростей Рэлея), можно сделать вывод, что наилучшая гомогенная адгезия реализуется после отжига при 500°C.

Ключевые слова: неразрушающая диагностика, сканирующий акустический микроскоп, механические свойства, эффекты отжига, тонкие плёнки Al/Si.

(Received December 11, 2017; last version—September 17, 2018)

1. THE ACOUSTIC MICROSCOPE

1.1. The Transducer

In 1970, Quate and Lemons developed, at Stanford University, the first scanning acoustic microscope (SAM) [1–4]. The most prominent component of this microscope is the transducer (a piezoelectric thin film of, typically, ZnO or $LiNbO_3$). It produces a frequency that depends on its thickness. The role of this transducer is to convert a high frequency electrical signal into an ultrasound wave, which propagates with the same frequency (as the electrical signal) along a small rod of quartz or sapphire that acts as an acoustic delay line (Fig. 1).

1.2. The Lens

An acoustic beam generated at one face of this rod is focused by a spherical, cylindrical or conical cavity cut into the other face of the rod, which acts, then, as a lens [5–9]. This type of lens is object-dependent and has given birth to a phenomenon in acoustic microscopy, to which a ‘great interest’ is dedicated: the development of quantitative elastic measurements.

Normally, spherical lenses are used for acoustic surface imaging, since the spherical aberration can be neglected in this case.

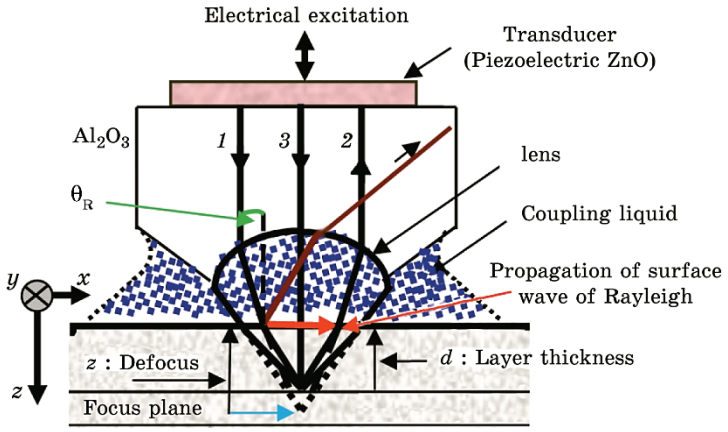

Fig. 1. Schematic configuration of the piezoelectric transducer in reflection scanning microscope. Rays *1* and *2* represent respectively axial and Rayleigh leaky waves; ray *3* represents specular wave.

In bulk imaging, a convergent beam is refracted at the sample surface prior to focusing below the surface. Such refraction occurs off normal and generates aberrations that can be significant even for small angles of observation.

However, the use of spherical lenses that eliminate aberration effects and achieve rigorous convergence of the acoustic beam at deeper levels in the bulk can easily solve this problem.

Moreover, in anisotropic materials, the fact that the surface wave velocity depends on the direction of propagation makes the spherical lenses unsuitable for the study of these materials: they can only help adjust the final experimental results [5].

However, cylindrical lenses that allow, at a given time, making elastic measurements in one direction are usable for the study, with a certain precision, of these materials.

This technique is also known as the line-focus beam technique [5].

Lamb's modes and interfacial weakness detection in multilayer systems were recently investigated using conical lenses. The last generate conical wave fronts that have a single angle of incidence on the specimen [10]. The description, on the other hand, of the mathematical procedure for acoustical lens design is available in the literature [11–15].

1.3. The Coupling Liquid for Lens to Sample Signal Transmission

Because the high-frequency acoustic waves do not propagate in the air, the use of a coupling liquid is necessary for acoustical signal transmission from lens to sample; this fluid plays also an important role in the

TABLE 1. Acoustic parameters of water and mercury [16–18].

$T = 298$ K	Velocity, m/s	Density, $10^3 \cdot kg/m^3$	Impedance Z, Mrayl	Attenuation α, $dB/(mm \cdot GHz^2)$
Water	1497	1	1.494	191
Mercury	1450	13.53	19.7	50

determination of the resolution of the acoustic microscope.

The attenuation in the liquid, on the other hand, determines the highest frequency (and, therefore, the shortest wavelength) that can be used and, thus, the best resolution that can be achieved.

At frequencies (f) higher than 10 MHz ($f > 10$ MHz), almost all fluids experience an attenuation that is proportional to the square of the frequency.

However, the majority of applications employ water and mercury because of their respective advantages (Table 1).

1.3.1. The Advantages of Water

Water has two advantages: a very weak attenuation at room temperature (approximately 191 dB/mm at 1 GHz) that decreases to reach 95 dB/mm at 60°C, and a good compatibility with most materials. Table 1 presents the principal acoustic parameters of water and mercury.

1.3.2. The Advantages of Mercury

Mercury also has an attractive attenuation coefficient at room temperature. However, the main advantage of this liquid metal is its high acoustic impedance. This valuable property allows good impedance matching to solid samples, which, in turn, allows surface examination by imaging.

Mercury also ensures a good signal transmission at the lens–liquid and liquid–solid interfaces [16–18].

1.4. The Two Modes of the Acoustic Microscope

The acoustic microscope can work in two modes: the reflection and transmission modes.

1.4.1. The Reflection Mode

In reflection mode, the SAM operates with a single transducer for

transmitting and receiving the acoustic signal, thus, resembling a miniradar or sonar system.

1.4.2. The Transmission Mode

In the transmission mode, however, the use of two transducers symmetrically arranged with respect to the sample under investigation is necessary.

In this case, one obtains the acoustic image of an object, located in a plane parallel to the sample surface, by scanning mechanically the sample in two perpendicular directions (x, y) relative to the transducer collecting the amplitude of the transmitted or reflected beam and displaying the collected amplitude on the screen of the microscope mapping apparatus.

The magnification of the scanning field can be varied from 3 to 3000.

The microwave electronics is necessary to acquire and process the acoustic signal [1, 10, 11].

1.5. Usefulness

Finally, we note that SAM gives information about the elastic properties of the material under investigation. The contrast in the acoustic images being due to variations in elasticity and density as well as to acoustic attenuations in the material. Consequently, this microscope is particularly suitable for the study of optically opaque materials, for which the usual optical techniques of characterization fail.

2. ACOUSTIC CHARACTERIZATION

The acoustic signal that originates from the sample is the result of the superposition of several types of waves that interfere at the transducer level.

By varying the lens aperture $\theta = 50°$, it is possible to generate, within a specimen, either one or several modes, those that propagate with their own specific velocities.

As z varies, the phases of these waves change at different rates; so, they can alternate between constructive and destructive interference.

Under these conditions, the output voltage $V(z)$ produced by the transducer presents (pseudo-oscillations) constitute the acoustic material signature.

Figure 2 presents an example of the experimental acoustic signature $V(z)$ for aluminium sample with use a water as the coupling liquid at 600 MHz.

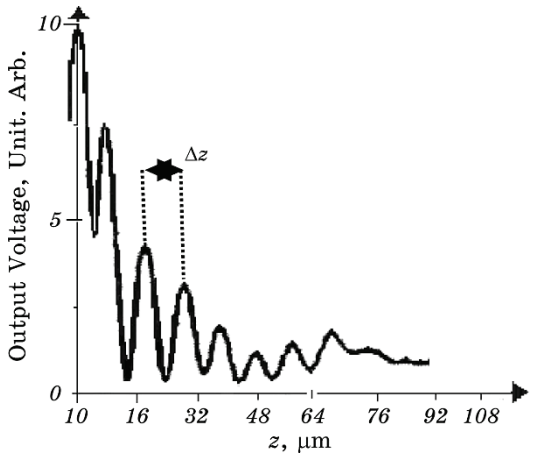

Fig. 2. Acoustic signature $V(z)$ for water/Al at 600 MHz.

Quate [1] gave the first theory of the $V(z)$ acoustic signature, which consisted in decomposing the waves (pseudo-oscillations) into frequency spectra and (then) analysing them by Fourier optics.

However, the theoretical model for the $V(z)$ effect proposed by Shepard and Wilson [19] gives (different) expressions that are easier to program and that based on the propagation of the acoustic field.

According to this model, the following expression gives the amplitude of the $V(z)$ signature:

$$V(z) = \int_0^{\theta_{max}} P^2(\theta) R(\theta) \exp(2jk_0 z \cos\theta) \sin\theta \cos\theta d\theta, \qquad (1)$$

where $j = \sqrt{-1}$, θ_{max} is the opening angle of the lens, $P^2(\theta)$ is the lens pupil function, $R(\theta)$ is the reflectance function of the specimen, and k_0 is the wave number in the coupling liquid.

Equation (1) shows that when the specimen is 'defocused' (*i.e.*, shifted) by an amount z, the resulting phase difference is $2k_0 z\cos\theta$.

We note that the function $R(\theta)$ is easily expressible for massive materials. However, in the case of layered structures, the reflectance function is more complex, and the Brekhovskikh model must be used to get it [20].

The Rayleigh wave is the surface acoustic wave that contributes most to the $V(z)$ interference curve. It results from the superposition of longitudinal and shear waves, which travel along the surface with a same phase velocity V_R; this V_R is, however, smaller than the velocity for the other wave kinds that may be present in the bulk [16–21]. In the particular case of isotropic solids, this wave consists of two components: the longitudinal and the shear components. These are $\pi/2$ out of

phase and are contained within the sagittal plane, *i.e.*, the plane defined by the wave vector normal to the solid surface. The dependence $V(z)$ permits to determine the velocity of the Rayleigh waves, V_R, in the specimen surface, a quantity that is related to the operating frequency f of the SAM, to the periodicity Δz of the resulting oscillations in $V(z)$ and to the wave velocity V_0 in the coupling liquid. This velocity is given by:

$$V_R = V_0 \left(1 - \left[1 - \frac{V_0}{2f\Delta z} \right]^2 \right)^{1/2} . \tag{2}$$

The period Δz (defined as the motion in the z direction needed for an angular change of 2π in the relative phase) is expressed in terms of the wavelength (λ_0) within the coupling liquid and the Rayleigh angle (θ_R) by:

$$\Delta z = \frac{\lambda_0}{2(1 - \cos\theta_R)}, \tag{3}$$

where θ_R is given by Snell's law, *i.e.*, $\sin\theta = V_0/V_R$. Here, V_R is expressible in terms of the longitudinal and shear wave velocities of the material (*i.e.* V_L and V_T) using an expression deduced from the reflective power [7, 11] (see Eq. (4)), where ρ_s is the density of the material to be examined:

$$4\left(\frac{V_T}{V_R}\right)^{1/2}\left(1 - \frac{V_T^2}{V_R^2}\right)\left(\frac{V_T^2}{V_L^2} - \frac{V_T^2}{V_R^2}\right)^{1/2} + \left(1 - 2\frac{V_T^2}{V_R^2}\right)^{1/2} = \left(\frac{\rho_0}{\rho_s}\right)\frac{\frac{V_T^2}{V_L^2} - \frac{V_T^2}{V_R^2}}{\frac{V_T^2}{V_0^2} - \frac{V_T^2}{V_R^2}}. \tag{4}$$

3. CHARACTERISTICS OF THE SAMPLES

The analysed sample was a segment ($\Phi = 12$ cm) of an aluminium-coated silicon wafer with (100) crystallographic orientation. The aluminium layer was deposited *via* vacuum evaporator Balzers BA510 is 10 μm, and its thickness was determined *via* profilometry. In addition, the density of the aluminium thin film was determined as 2.709 g/cm^3 *via* X-ray diffraction using a D8 Discover system (Bruker, Billerica, MA, USA).

The desired effect through the process of annealing the layer of Al/Si is to find the optimal conditions for having a homogeneous thickness of aluminium on the substrate in silicon [100], and in particular on a surface of (5×5 cm) without any chemical reaction between

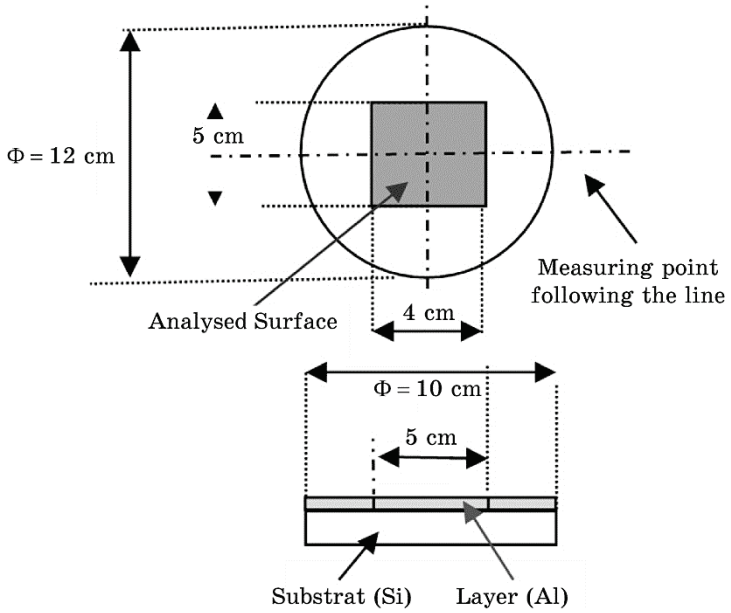

Fig. 3. Silicon wafer with uninterred aluminium layer.

aluminium and silicon (Fig. 3), in addition, the objective of this study is to prepare the supports in Al/Si that will serve for other specific applications requested by an industrialist.

The acoustic sensor (delay line of SiO_2 and layer of transducer in ZnO) used in this work is manufactured in our LEAM laboratory: *1*—after mirror polishing of the upper part of the SiO_2 delay line, the lens is made whose diameter is a function of the frequency; *2*—the deposition of the different layers is carried out in a Balzers BA 510 evaporator; *3*—assembling the sensor and fixing the connectors; *4*—control of the working frequency is set using an HP brand network analyser.

Rayleigh and transversal speeds are calculated after each acquisition of an acoustic signature $V(z)$ along a wafer line of 12 cm in diameter with a pitch of 10 mm, and this after the acquisition of images (Fig. 4).

The treatment of the $V(z)$ by fast Fourier transform (FFT) allows us to calculate the different speeds that interact in the material.

Figures 5 and 6 represent the dispersion of the speeds measured at 600 MHz; we notice: a discontinuity of the curve at 400°C along the length of the measurement line. That it is not constant at 600°C, it is constant at 500°C.

The discontinuity and the non-constant of the curves is probably due to either a detachment of the layer of aluminium against the substrate (blue contrast Figs. 4, *c*, 6 and 7), or to a default of adhesion.

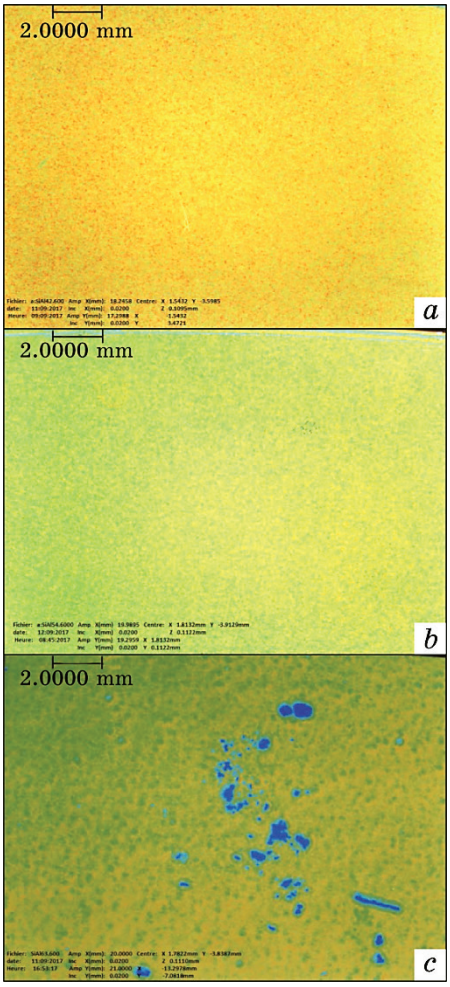

Fig. 4. Acoustic images of the interface of the system Al(10 μm)/Si[100]; coupling liquid water, $f = 600$ MHz, temperatures of annealing: 400°C (*a*), 500°C (*b*) and 600°C (*c*).

Table 2 summarizes the treatments given to four samples in our study. These have undergone a preliminary metallization at 500°C. We carried out the study on a series of samples under the same temperature (24°C) conditions in all cases.

4. RESULTS AND DISCUSSIONS

Figure 4 gives acoustic images taken at the layer/substrate interface with water as coupling fluid and with a spherical lens with a 50° open-

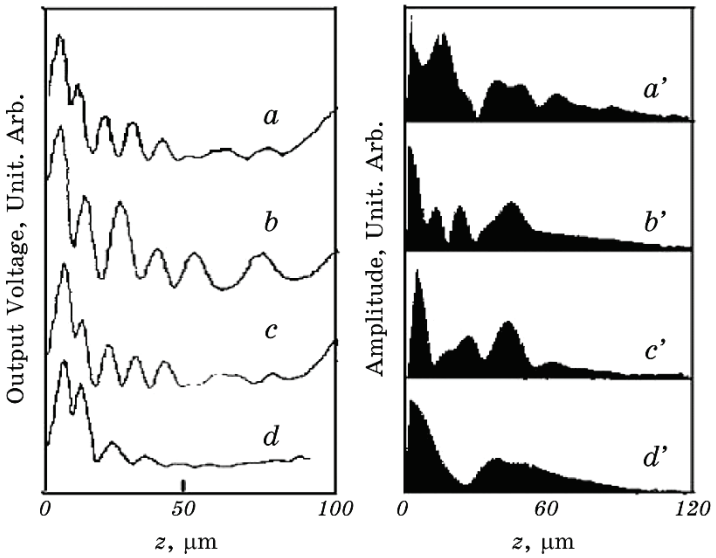

Fig. 5. Acoustic signature $V(z)$ and FFT spectrum for water/Al(10 μm)/Si at 600 MHz.

ing.

A first instance analysis of the images given in Figure 4 enables us to discuss the ensemble of the samples that have undergone annealing at 600°C. These present also a non-uniform contrast embodied by dark spots (that represent, for instance, short-circuit, separation, *etc.* and that are related to the preparation method used); see Fig. 4, *c*.

The results, obtained after treatment of the acoustic signature and the calculation of the propagation velocity, strengthen the choice of the temperature used, *i.e.* 24°C.

Indeed, on the one hand, we obtain an acoustic signature that is stronger in the uniform regions and that is more attenuated in the dark spots; this is confirmed by the results obtained by means of the FFT (Fig. 5, *d*′). On the other hand, Figs. 5 and 6 show significant speed dispersion.

We note at this point as follow.

1. We discarded all reference samples (that have undergone an annealing at 400°C) that presented significant dispersion speeds V_R and V_T (Figs. 6 and 7).

2. Only the samples, among those that have undergone an annealing at 500°C, that are characterized by (i) homogeneous images on all surfaces (Fig. 1, *b*), (ii) an acoustic signature $V(z)$, (iii) a signal that is exploitable by FFT (Fig. 5, *c*′) and (iv) practically constant dispersion speeds (Figs. 6 and 7) will be maintained for possible studies and/or applications.

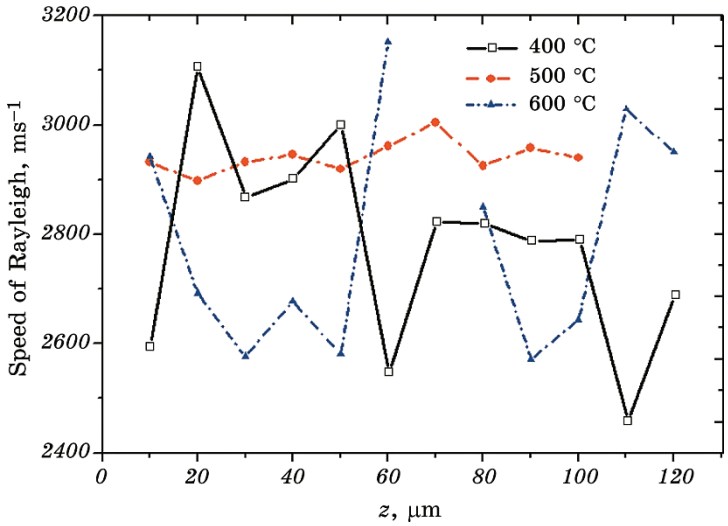

Fig. 6. Dispersion of Rayleigh speed for the system water/Al(10 μm)/Si[100] at 600 MHz.

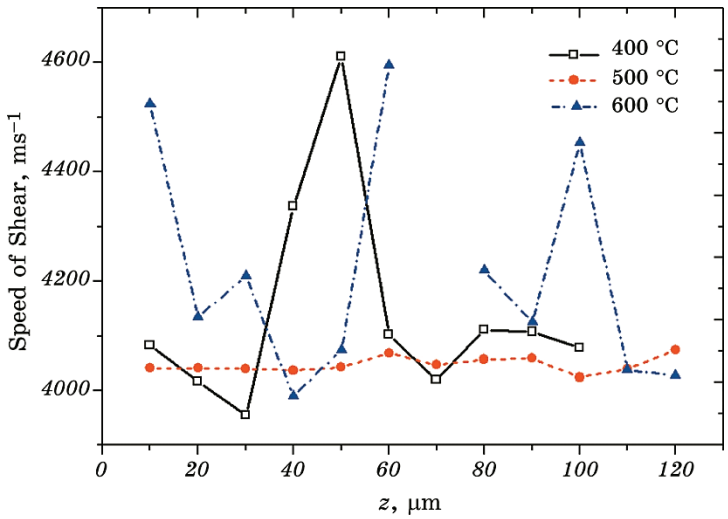

Fig. 7. Dispersion of shear velocity for system water/Al(10 μm)/Si[100] at 600 MHz.

3. Here, we consider the interfaces as homogeneous whenever they do not give rise to interference phenomena.

4. We based the acoustic microscope calibration on the 256 colours levels, the red colour corresponding to a perfect layer/substrate adherence. On the other hand, the blue colour that one can observe in Fig. 4,

TABLE 2. Characteristics of samples Al(10 μm)/Si[100].

No. of sample	*T* of annealing, °C	Chemical attack
A	No	Yes
B	400	–
C	500	–
D	600	–

c (dark holes) corresponds to a complete substrate/layer separation (and thus, is indicative of maximum signal attenuation).

5. It is possible, using an appropriate model for adherence between two materials, to compute the reflection coefficient $R(\theta)$ (in module and in relative phase) for good as well as for bad adhesion when the medium is a multilayered one.

6. It is not in the aims and purposes of this paper to consider the development of the theory of rigid and smooth bonding; this one can be found in more fundamental papers [7, 11]. Instead, it is intended here to extract the results that are most significant for the design of a transducer for acoustic microscopy.

5. CONCLUSIONS AND PROSPECTS

The acoustic microscope with a frequency range from 100 to 600 MHz seems to be a powerful tool for non-destructive testing. It not only makes it possible to detect defects whose dimensions are lower than 50 μm, but also gives an image that can facilitate their interpretation and control.

In addition, the possibility that this apparatus gives for evaluating and studying the defects that develop during the annealing process makes of it a very precious tool indeed.

The present results show that the acoustic microscopy is a control tool with performances and flexibility that are particularly well adapted for performing non-destructive tests. It can become a complementary and/or essential tool for the local mechanical characterization of materials placed in hostile environments.

Although the obtained experimental results agree with the theoretical ones, there remain a few extra points that need further development (*i.e.*, in order to improve the possibilities and capacities of this method); these are:

– taking into account the effects of attenuation (longitudinal and/or transversal) in theoretical calculations to get closer to reality (that which is imposed by the actual experimental conditions);

– studying more deeply the opposite phenomenon-related approach;

– looking further into the study of the linear prediction of the acoustic signature;

– establishing prototypes (references) that may be used as standards in the quality control process;

– developing a way (*e.g.*, a digital one) of processing acoustic images in order to make their interpretations easier.

The authors wish to express very warm thanks to their colleague N. Hadji, from the Department of Physics, for his valuable help in preparing the English version of this paper.

REFERENCES

1. R. A. Lemons and C. F. Quate, *Appl. Phys. Lett.*, **24**: 163 (1973).
2. R. A. Lemons and C. F. Quate, *Appl. Phys. Lett.*, **25**: 251 (1974).
3. R. A. Lemons and C. F. Quate, *Physical Acoustics*, **14**: 1 (1979).
4. A. Briggs, *Advances in Acoustic Microscopy* (New-York: Plenum Press: 1995).
5. J. I. Kushibild and N. Chubachi, *IEEE Trans. Sonics Ultrason.*, **SU-32**: 189 (1985).
6. J. D. Achenbach, J. O. Kim, and Y.-C. Lee, *Advances in Acoustic Microscopy. Volume 1* (Ed. A. Briggs) (New York: Plenum Press: 1995), p. 153.
7. R. J. M. da Fonseca, L. Ferdj-Allah, G. Despaux, A. Boudour, L. Robert, and J. Attal, *Advanced Materials*, **5**, Nos. 7/8: 508 (1993).
8. A. Atalar, H. Köymen, and L. Degertekin, *IEEE Ultrasonic Symposium Proceedings* (Piscataway, NJ, USA: EEE Service Center: 1990), p. 359.
9. B. Cretin and F. Stahl, *Appl. Phys. Lett.*, **62**: 829 (1993).
10. A. Atalar, H. Köymen, and F. L. Degerteidn, *IEEE Trans. Ultrason., Ferroelect., Freq. Contr.*, **39**: 661 (1992).
11. A. Boudour, *Etude par Microacoustique des Différents Modes de Propagation Dans les Structures Monocouches et Multicouche* (Thesis of Disser. ... for Dr. Sci.) (Annaba: Université Badji Mokhtar Annaba: 2000) (in French).
12. H. Lazri, E. Ogam, A. Boudour, Z. E. A. Fellah, A. Oduor, and P. Baki, *Ultrasonics*, **81**: 10 (2017).
13. A. Boudour, Y. Boumaiza, M. Guerioune, and S. Belkahla, *phys. status solidi (a)*, **201**, Iss. 1: 80 (2004).
14. A. Boudour, S. Deboub, T. Tahraoui, M. Ramdani, and Y. Boumaiza, *PICMS AMSE (MS'07 Algeria) (July 2–4, 2007)* (Algiers: 2007).
15. B. Cros, *Rev. Met. Paris*, **98**, No. 2: 215 (2001).
16. J. Attal, *Scanned Image Microscopy* (Ed. E. A. Ash) (New York: Academic Press: 1980), p. 97.
17. J. Attal, C. Amaudric Du Chaffaut, K. Alami, H. Coelho-Mandes, and A. Saied, *Electronics Letters*, **25**, No. 24: 1625 (1989).
18. A. Doghmane, Z. Hadjoub, K. Alami, J. M. Saurel, and J. Attal, *J. American Society of Acoustic*, **92**: 1545 (1992).
19. C. J. R. Shepard and T. Wilson, *Appl. Phys. Letters*, **38**: 858 (1981).
20. L. M. Brekhovskikh and O. A. Godin, *Acoustic of Layered Media I: Plane and Quasi-Plane Waves* (Berlin: Springer-Verlag: 1990).